

Improving Geomorphological Classification via Binary Image Processing

A. Camila Salgado-Albiter

Facultad de Ciencias

Universidad Nacional

Autónoma de México

Ciudad de México, México

camila.salgado@ciencias.unam.mx

S. Ivvan Valdez

Observatorio Metropolitano

Centro de Investigación en

Ciencias de Información Geoespacial A.C

Querétaro, México

svaldez@centrogeo.edu.mx

Jorge Paredes-Tavares

Observatorio Metropolitano

Centro de Investigación en

Ciencias de Información Geoespacial A.C

Querétaro, México

jparedes@centrogeo.edu.mx

Abstract—Landform classification is the basis for understanding and describing the processes and evolution of landscape. This process usually requires elevation information from different sources, expertise and time. Automatic geomorphological classification, via the geomorphons algorithm, supports expert classification by using local ternary patterns for labeling landform elements, significantly reducing the computation time. Nevertheless, it presents issues such as a noisy output, valleys that are not classified as continuous forms, valleys that are classified as peaks at low altitude, flat zones inside the valley that are not classified as a part of it, and other similar issues. In this proposal, we tackle the mentioned issues for valley classification by binarizing the geomorphons output and applying it binary-image operators. The proposal's performance is measured by using binary classification metrics and expert-made groundtruth images. The results show that the accuracy, balanced accuracy, and F1 metrics are greater than those delivered by the geomorphons classifier for all the instances in the testing data.

I. INTRODUCTION

Landform classification is the basis for understanding and describing the processes and evolution of landscape. It plays a significant role in geomorphological mapping and it has applications in hydrology, ecology, geology, assessment of natural hazards, land-use planning, among others [35], [18], [34], [13]. Landform mapping has relied heavily in the empiric interpretation of topographical maps and aerial photographs and it is a labor-intensive and time-consuming task [24]; nevertheless, the increasing availability of Digital Elevation Models (DEM) have encouraged the research on automatic landform classification [15].

Automatic landform classification have been approached by measuring and quantifying general and specific geomorphometric characteristics [24]. This was first stated by Evans (1972) [7] who defined general geomorphometry as the study of continuous land surface and specific geomorphometry as the analysis of geometric and topological characteristics of landforms [8]. For this matter, general geomorphometry classification is focused on sub-components of landforms, which are relatively homogeneous with respect to their *shape*, *steepness*, *orientation* and *relative landform position* [22].

The existent methods for automatic classification of landform elements include pixel-based [14] and object-based [6], and machine-learning techniques [10], [21].

The geomorphons classifier proposed by Jasiewicz & Stepinski (2013) [16] uses the concept of Local Ternary Patterns (LTP), which was first introduced by [33], for the classification of local patterns in face recognition. Jasiewicz & Stepinski (2013) [16] focused this concept to identify ten of the most common local landform elements called *geomorphons*. These include the elements *ridge*, *peak*, *shoulder*, *spur*, *slope*, *footslope*, *flat*, *hollow*, *valley* and *pit*. Geomorphons is topic of research for prediction of specific landforms and landscape evolution[20], [9], [32]; accuracy assessment between surveyors classification and other automatic methods[19], [12]; and it was applied in pedology, land-use planning and watershed hydrology [25], [2], [4], [36].

Nevertheless, current approaches present some disadvantages to be comparable with human classification such as noisy classification, that is to say single pixels of class A surrounded by pixels of class B and incorrect classifications according to its elevation, such as landforms classified as valleys in highlands while peaks and ridges are in low-lands. Finally, another issues is valley classification in drainage basins, which does not preserve its continuous structure and is classified as a short formation [23]. This work deals with the previous issues by applying binary image-processing operators, this proposal significantly improves the geomorphons classification as it is evidenced by classification metrics, using as ground truth a human classification.

II. METHODOLOGY

We introduce a method for improved valley classification using binary operators, named as the Binary-based Geomorphons Improvement (BOGI). The proposal uses as a basis a landform classifier proposed in [16], named as geomorphons, via the implementation developed in [11]. Therefore, the Binary-based Geomorphons Improvement (BOGI) combines the application of the *geomorphons* method and binary image processing to improve valley classification. A general outline of this proposal is shown in Figure 1. The **input** is a DEM, the geomorphons method is applied on it, then the resultant raster is binarized by setting the *footslope*, *valley*, *pit* and *hollow* to 1, and the remaining classes to 0. The resultant binary image is processed by means of applying a stack of binary operators such as

a median filter and *erosion*, *dilatation*, *opening* and *closing*. At last, the output is the proposal which contains a binary improved valley classification.

For evaluating the effectiveness of the BOGI method we compared it to the original geomorphons method via widely-used and appropriate performance metrics for binary classifiers.

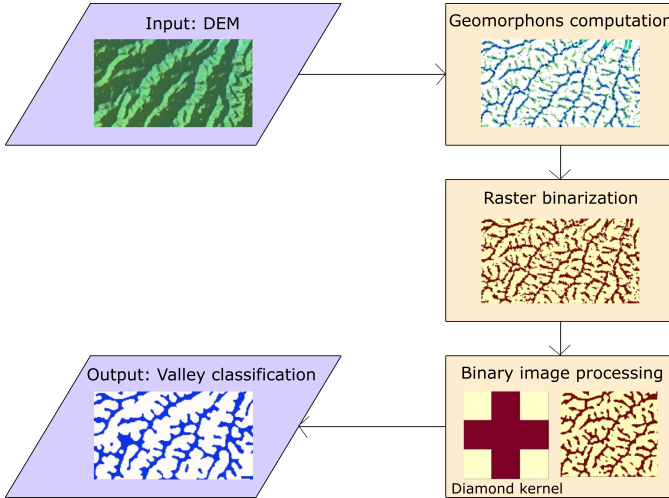


Fig. 1. General flowchart of the Binary-based Geomorphons Improvement (BOGI).

A. Data acquisition

1) *Case of Study* : The area of study is located in the State of Mexico between the coordinates $19^{\circ} 44' 58''$ and $19^{\circ} 51' 4''$ N latitude, $99^{\circ} 28' 49''$ and $99^{\circ} 20' 0.7''$ W longitude (Fig. 2). It covers approximately 170 km^2 in the draining area of the Taxhimay dam. The region is primarily composed of alluvial material, basaltic and andesitic lava, and epiclastic rocks of Pleistocene age. The topographic forms are hills and mountains formed by volcanic activity. A fault system controls the drainage network [5]. A Digital Elevation Model (DEM) of the study area was obtained from the Digital Elevation Collection of USGS with a 30 m resolution [1]. The DEM was cropped to 9 separate windows of 171×121 pixels.

B. Geomorphons Computation

The geomorphons implementation was developed by [11] based on the proposed method of [16] in the programming language R. There are three inputs needed for this process: a DEM and two scalar parameters. The latter were set as default by the implementation previously mentioned. These two parameters control the extension and flatness of the landform classification: lookup distance L and flatness threshold t . The lookup distance L is set to 7 pixels, which determines the maximum size of the landform element. Furthermore, the flatness threshold t is set to 1 degree, meaning the maximum slope of the flat terrain in the classification. The output is a raster file with the classification of the landform elements above-stated.

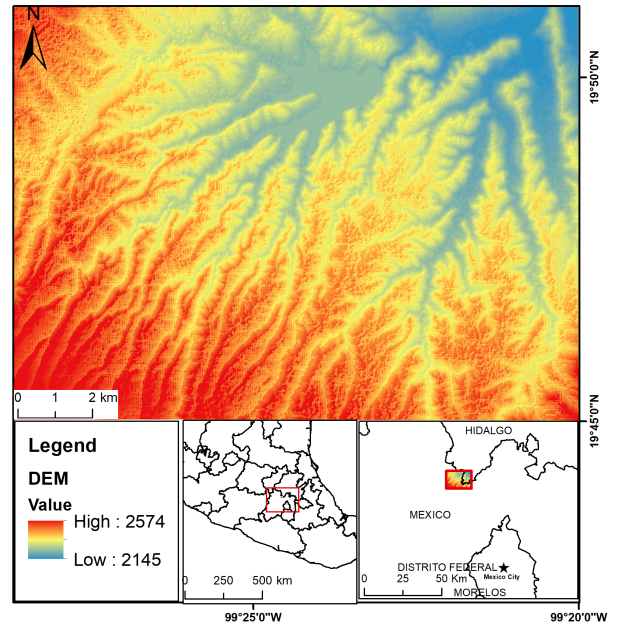


Fig. 2. Study area used for the landform classification.

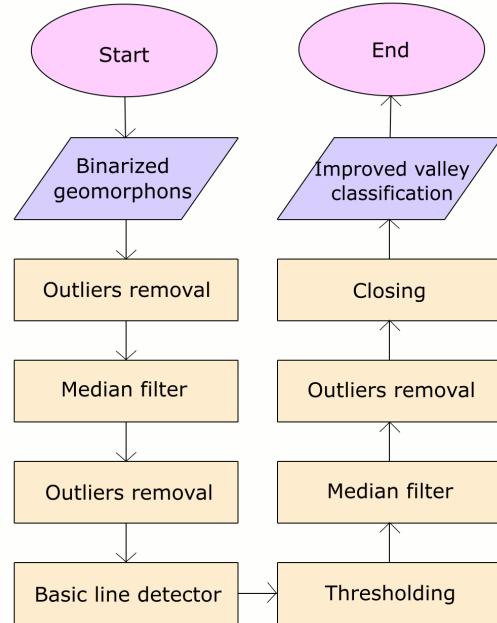


Fig. 3. Flowchart of the binary image processing for developing the improved valley classification

C. Binarization

Straumann & Purves [30] defined valleys low areas or depressions relative to their surroundings, they are elongated, and have a gentle slope and often contain a stream or river. Additionally, they are integrated by a valley floor which is a relatively broad, flat region within a valley [30]. Hence, following this definition, the geomorphons labels used in the

proposal are the landforms *footslope*, *valley*, *hollow* and *pit*. These labels are set to 1, otherwise to 0.

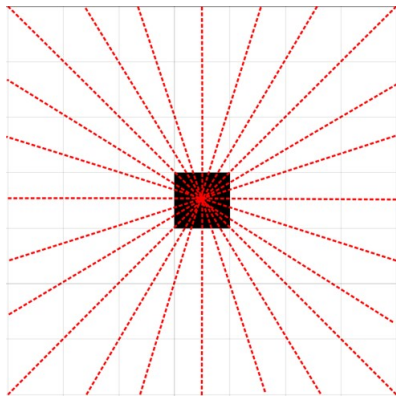


Fig. 4. Line detector in a window of 7×7 .

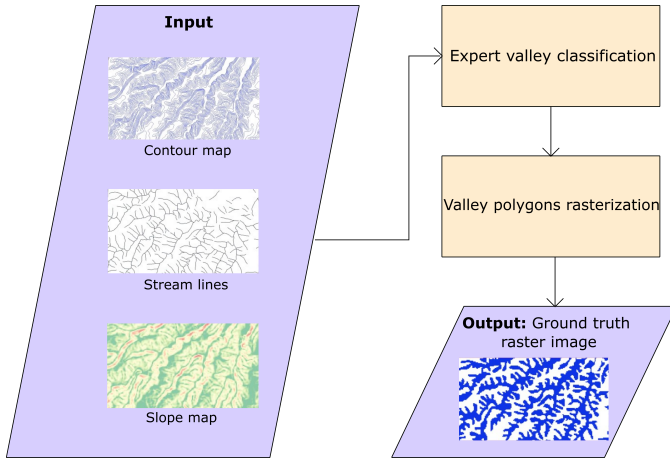


Fig. 5. Flowchart for obtaining the ground-truth drainage network

D. Improving geomorphons classification via binary image processing

The algorithm developed for obtaining the improved valley classification is shown in Fig. 3.

The binary image processing includes widely-used binary morphological operators such as *dilatation*, *erosion*, *closing* and *opening* [29] and median filtering. Additionally, the method comprises specialized operations such as *thresholding*, an outliers removal, and the *basic line detector* first introduced in [28].

1) *Outliers Removal*: The outliers are removed using overlapped windows, the pixels in the window are used to compute the mean and standard deviation in Equation (1), to compute a threshold, the pixels above such threshold are considered as outliers and the valley label is unset.

$$x(p, \sigma, \mu) = Q(p)\sigma + \mu \quad (1)$$

In the computation of the outlier threshold, x , Q is the p percentile of a normal distribution $N(\mu, \sigma)$ which parameters

μ and σ are estimated from the elevation values z . If $z > Q(p)\sigma + \mu$, then, the pixel with elevation z is reset to a value of 0, that means that the class label is removed, and the pixel has not an assigned class. Otherwise, the pixel keeps its value of 1.

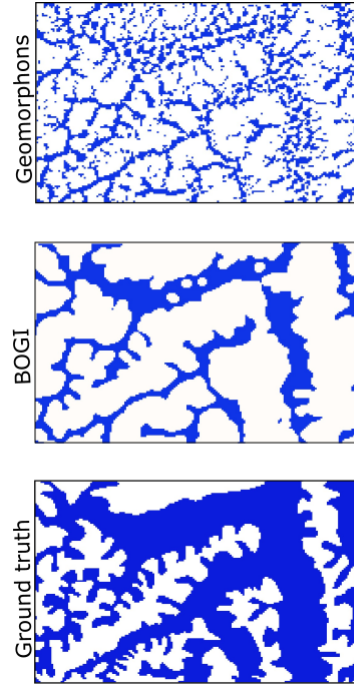


Fig. 6. Aggradation zones present in the area of study. Comparison between geomorphons, BOGI and groundtruth.

2) *Basic Line Detector*: We apply the basic line detector proposed by [28] for retinal blood vessel segmentation illustrated in Fig. 4.

This detector overlaps a set of lines in twelve orientations over a window of 7×7 pixels of the binary image, each line is used as a mask and the sum of the overlapped pixels is computed for each line, the maximum sum is returned as the corresponding value of the central pixel of the window.

3) *Thresholding* : For binarizing the grey-scale image computed from the basic line detector, a threshold is obtained by the Otsu's method from the R package EBImage [26]. The pixels with values greater or equal than the threshold are set to 1, otherwise, it is set to 0.

4) *Additional binary operators* : The other binary operators we apply are from the R package EBImage [26] which contains tools for image processing and analysis. This package includes the median filter and the erosion, dilatation, opening and closing.

III. GROUND TRUTH AND PERFORMANCE METRICS

The ground truth is generated according to the outline showed in Fig.5. A trained person draws polygons of the valleys in the area of study using QGIS software [27]. This delimitation uses a slope map, stream line and contour map.

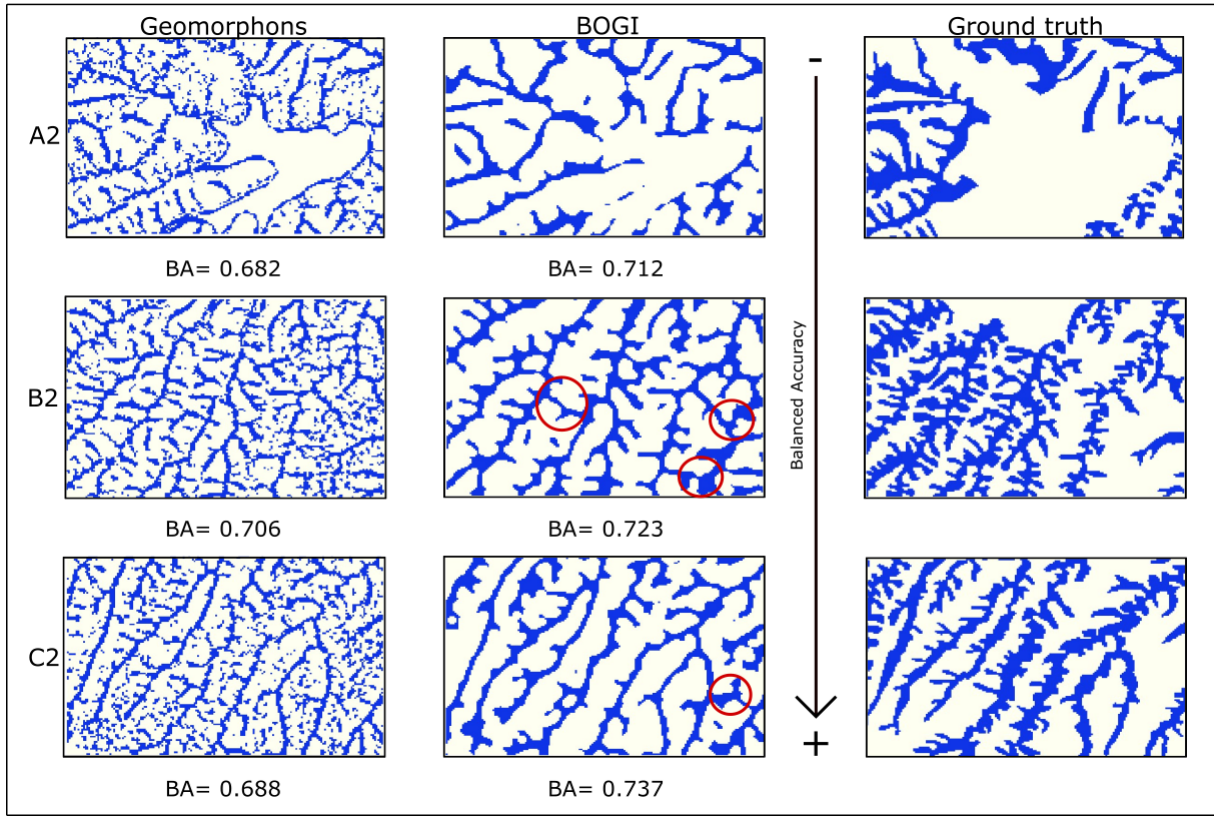


Fig. 7. Comparison of geomorphons and BOGI method to the groundtruth.

Then, the valley vector data is rasterized and cropped in 9 separate windows of 171×121 pixels for performance assessment purposes.

To evaluate the performance of the BOGI method we compare it with the geomorphons classifier, using some of the most used performance metrics for binary classifiers. First, we calculate the two metrics *Sensitivity* and *Specificity* which are useful for measuring the prediction success of the positive class and negative class, respectively. We also make use of the metric *Accuracy* which divides the total correct predictions by the total predictions [3]. However, the data present has an imbalanced class distribution, meaning that the presence of 0 prevails above 1, the *Accuracy* is not adequate because it can lead to biased conclusions [3], [17], [31]. Hence, we use the *Balanced Accuracy* and the *F-score* which are recommended for imbalanced data as they provide more reliable information [24].

1) *Ground truth data*: Regarding to measuring the performance of the proposal we compare it to the geomorphons method. The valley ground-truth tracing uses an elevation contour map, a stream line and a slope map of the site of study (Fig. 5). For standardizing the delimitation of the valley landform, we followed a set of rules:

- Follow the direction of the convex contours and stream lines.
- Include in the delimitation the zones with 40 or more

slope.

- Beware of the concave contours belonging to ridge zones to adequately set the valley boundaries.

IV. RESULTS AND DISCUSSION

A. Valley classification

The comparison of the classified valleys using geomorphon and BOGI methods, and the ground truth is shown in Fig. 7. One of the main differences between the two methods is the noise reduction by the BOGI method, since geomorphons only focus on the pattern recognition of elevation values. This drawback is circumvented with the application of the outlier removal by the BOGI method, additionally, it prevents the propagation of errors to the following operators.

In the same regard, the BOGI method joins corresponding valley structures that are disconnected in the geomorphons method, also, it widens the valley structures. This is attributed to the basic line detector and morphological operator *closing*. Nevertheless, it fails in some areas where different tributary valleys are very close to one another. The latter can be noted in the red circled areas in Fig. 7 where BOGI disrupts the dividing ridge by joining the valley structures.

In addition, the aggradation zones are better identified with the BOGI method. As this valleys have a really wide floor it is possible that some pixels are classified as flat and causes wide areas of discontinuity between pixels. Figure 6 shows that

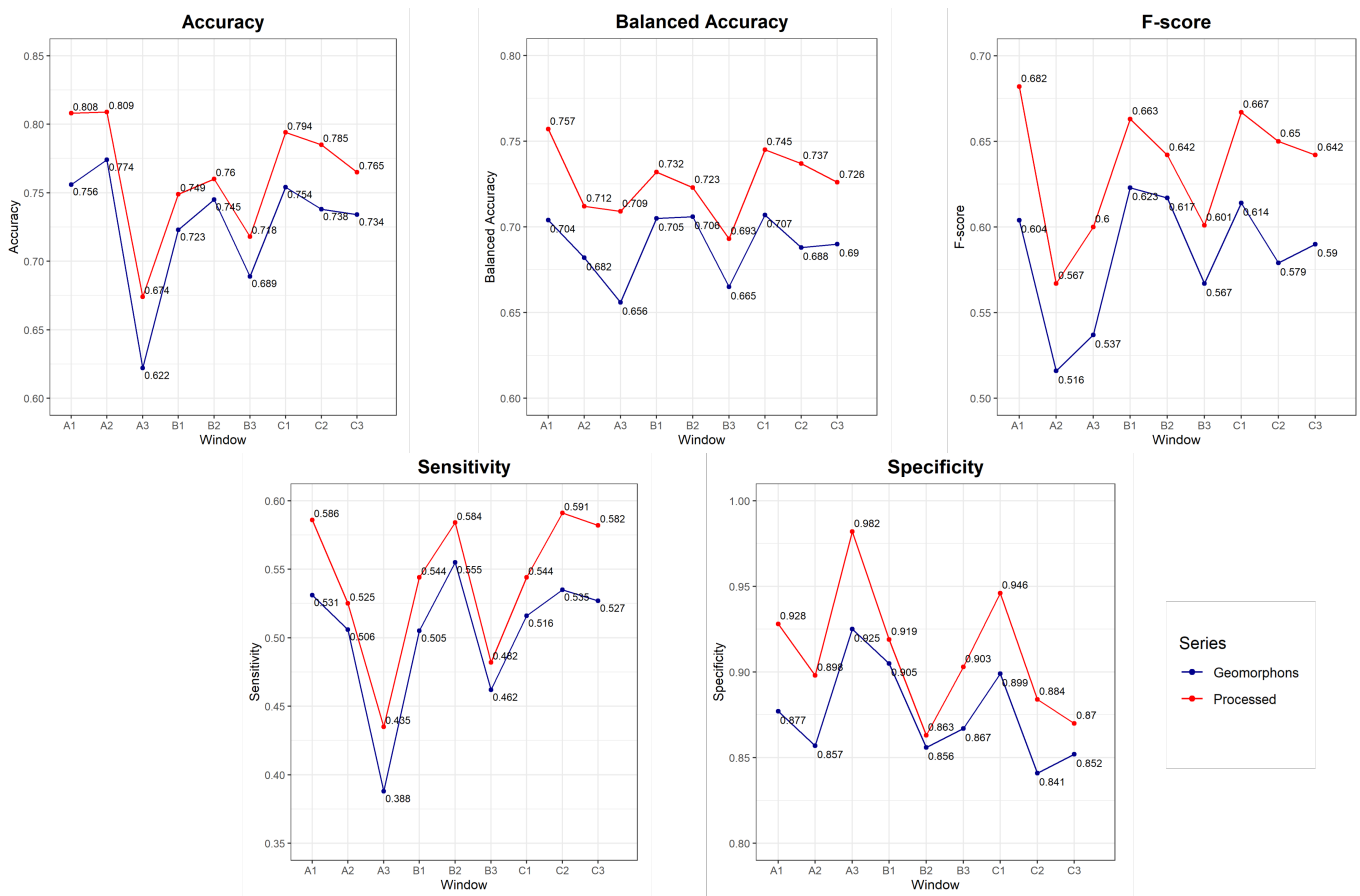


Fig. 8. Performance metrics for 9 testing windows, comparison of the geomorphons classifier versus BOGI. All metrics are improved for all cases.

BOGI enhance in some grade the extension of this alluvial plains but it is limited by the noisy classification done by geomorphons. Also, in window A2 we can note that geomorphons misclassify the surrounding area of the Taxhimay dam. This is due to the persisting slope declination where the class footslope dominates, nevertheless, BOGI reduces considerably this error. Finally, is worth mentioning that both geomorphons and BOGI don't classify valleys of reduce scale due to the resolution of the DEM.

B. Performance metrics assessment

The performance metrics *Accuracy*, *Balanced Accuracy* and *F1* are showed in Table I, and Fig. 8 we include a series of line charts of this same metrics with an addition of *Sensitivity* and *Specificity* to better visualize the comparison of geomorphons and BOGI method with respect of the ground truth.

In regards to the separate class metrics sensitivity and specificity, the BOGI method shows to be better at predicting the positive and negative classes than geomorphons in all 9 windows. It can be seen that the improvement in the sensitivity is lesser than the shown in the specificity. This is possible due to the missing small-scale tributaries and errors in the wide valley floors. Hence, we find the lesser sensitivity in windows A3 and B3 where we find the broader floor valleys. Besides,

there is a higher improvement in the specificity due to the outliers and noise removal previously mentioned. However, this proves that BOGI successfully removes important classifying flaws of geomorphons and enhances most of its pros.

Both methods present an accuracy greater than 70%. Nevertheless, the valley landform covers a relatively small proportion of the area of study and the no-valley class is dominant, thus, the accuracy metric is not reliable. Therefore, we shall focus on the other two performance metrics where the geomorphons and BOGI methods shows a mean of 68.9% and 72.6% for the Balanced Accuracy, and 58.3% and 63.5% for the F-score, respectively. In Fig. I we can see that BOGI has an increasing performance as we get further from the Taxhimay dam where we can find narrow valleys with shorter tributaries. On the contrary, BOGI struggles in low areas where the draining network is denser. Regardless, BOGI is better than geomorphons even in this windows with poorer performance.

V. CONCLUSIONS

In this work, we proposed a binary-based method for improving the automatic classification delivered by geomorphons. The main improvements of the proposed is the reduction of noisy pixels to avoid propagation errors, the extension of the true scale of the valley landform and its joint of

TABLE I
RESULTS OF THE PERFORMANCE METRICS. COMPARISON BETWEEN
GEOMORPHONS AND BOGI METHOD.

	Accuracy		Balanced Accuracy		F1	
	Geompn	BOGI	Geompn	BOGI	Geompn	BOGI
A1	0.756	0.808	0.704	0.757	0.604	0.682
A2	0.774	0.809	0.682	0.712	0.516	0.567
A3	0.622	0.674	0.656	0.709	0.537	0.600
B1	0.723	0.749	0.705	0.732	0.623	0.663
B2	0.745	0.760	0.706	0.723	0.617	0.642
B3	0.689	0.718	0.665	0.693	0.567	0.601
C1	0.754	0.794	0.707	0.745	0.614	0.667
C2	0.738	0.785	0.688	0.737	0.579	0.650
C3	0.734	0.765	0.690	0.726	0.590	0.642
Mean	0.726	0.762	0.689	0.726	0.583	0.635
Std	0.046	0.044	0.019	0.020	0.037	0.038

corresponding valley tributaries. This is supported by the performance assessment with the ground truth, where it shows to be greater than geomorphons in every metric. Even so, our method is limited in denser draining areas and by the initial classification of geomorphons where it omits small-scale valley tributaries. As this binary-based method was decided by visual expertise, in future works we could build a binary method based on greedy algorithms and explore the parameters of geomorphons with the approach of applying binary operators.

REFERENCES

- [1] "Science data catalog (sdc)." [Online]. Available: <https://data.usgs.gov>
- [2] J. Atkinson, W. de Clercq, and A. Rozanov, "Multi-resolution soil-landscape characterisation in kwazulu natal: Using geomorphons to classify local soilscape for improved digital geomorphological modelling," *Geoderna Regional*, vol. 22, p. e00291, 2020. [Online]. Available: <https://www.sciencedirect.com/science/article/pii/S2352009420300407>
- [3] M. Bekkar, H. K. Djemaa, and T. A. Alitouche, "Evaluation measures for models assessment over imbalanced data sets," *J Inf Eng Appl*, vol. 3, no. 10, 2013.
- [4] H. Chea and M. Sharma, "Residential segregation in hillside areas of seoul, south korea: A novel approach of geomorphons classification," *Applied Geography*, vol. 108, pp. 9–21, 2019. [Online]. Available: <https://www.sciencedirect.com/science/article/pii/S0143622818312517>
- [5] P. C. del municipio de Villa del Carbón, "Atlas municipal de riesgo de villa del carbón," 2016, accessed 28 april 2022. [Online]. Available: https://www.ipomex.org.mx/recursos/ipo/files_ipo3/2016/43031/9/905a66a2d38dd1fc78191add5bbe9a76.pdf
- [6] L. Drăguț and T. Blaschke, "Automated classification of landform elements using object-based image analysis," *Geomorphology*, vol. 81, no. 3-4, p. 330–344, 2006.
- [7] I. S. Evans, "General geomorphometry, derivatives of altitude, and descriptive statistics," *Spatial Analysis in Geomorphology*, p. 17–90, 1972.
- [8] ———, "Geomorphometry and landform mapping: What is a landform?" *Geomorphology*, vol. 137, no. 1, pp. 94–106, 2012, geospatial Technologies and Geomorphological Mapping Proceedings of the 41st Annual Binghamton Geomorphology Symposium. [Online]. Available: <https://www.sciencedirect.com/science/article/pii/S0169555X11001462>
- [9] L. Gawrysiak and W. Kociuba, "Application of geomorphons for analysing changes in the morphology of a proglacial valley (case study: The scott river, sw svalbard)," *Geomorphology*, vol. 371, p. 107449, 2020. [Online]. Available: <https://www.sciencedirect.com/science/article/pii/S0169555X20304220>
- [10] S. Ghosh, T. Stepinski, and R. Vilalta, "Automatic annotation of planetary surfaces with geomorphic labels," *IEEE Transactions on Geoscience and Remote Sensing*, vol. 48, no. 1, p. 175–185, 2010.
- [11] Z. R. A. GmbH and M. Sänger, "Landform classification in r," Aug 2018. [Online]. Available: <https://myweather.ch/blog/2018-08-22-landform-classification-in-r>
- [12] F. E. Gruber, J. Baruck, and C. Geitner, "Algorithms vs. surveyors: A comparison of automated landform delineations and surveyed topographic positions from soil mapping in an alpine environment," *Geoderma*, vol. 308, pp. 9–25, 2017. [Online]. Available: <https://www.sciencedirect.com/science/article/pii/S001670611730664X>
- [13] G. Hufschmidt and T. Glade, *Vulnerability analysis in geomorphic risk assessment*. Cambridge University Press, 2010, p. 233–244.
- [14] B. J. Irvin, S. J. Ventura, and B. K. Slater, "Fuzzy and isodata classification of landform elements from digital terrain data in pleasant valley, wisconsin," *Geoderma*, vol. 77, no. 2-4, p. 137–154, 1997.
- [15] J. Jasiewicz, P. Netzel, and T. F. Stepinski, "Landscape similarity, retrieval, and machine mapping of physiographic units," *Geomorphology*, vol. 221, pp. 104–112, 2014. [Online]. Available: <https://www.sciencedirect.com/science/article/pii/S0169555X14003110>
- [16] J. Jasiewicz and T. F. Stepinski, "Geomorphons — a pattern recognition approach to classification and mapping of landforms," *Geomorphology*, vol. 182, pp. 147–156, 2013. [Online]. Available: <https://www.sciencedirect.com/science/article/pii/S0169555X12005028>
- [17] L. A. Jeni, J. F. Cohn, and F. De La Torre, "Facing imbalanced data-recommendations for the use of performance metrics," *2013 Humaine Association Conference on Affective Computing and Intelligent Interaction*, 2013.
- [18] D. M. Kashian, B. V. Barnes, and W. S. Walker, "Ecological species groups of landform-level ecosystems dominated by jack pine in northern lower michigan, usa," *Plant Ecology*, vol. 166, no. 1, pp. 75–91, 2003. [Online]. Available: <http://www.jstor.org/stable/20146399>
- [19] T. Kramm, D. Hoffmeister, C. Curdt, S. Maleki, F. Khormali, and M. Kehl, "Accuracy assessment of landform classification approaches on different spatial scales for the iranian loess plateau," *ISPRS International Journal of Geo-Information*, vol. 6, no. 11, 2017. [Online]. Available: <https://www.mdpi.com/2220-9964/6/11/366>
- [20] Z. Libohova, H. E. Winzeler, B. Lee, P. J. Schoeneberger, J. Datta, and P. R. Owens, "Geomorphons: Landform and property predictions in a glacial moraine in indiana landscapes," *CATENA*, vol. 142, pp. 66–76, 2016. [Online]. Available: <https://www.sciencedirect.com/science/article/pii/S0341816216300030>
- [21] S. Lin, N. Chen, and Z. He, "Automatic landform recognition from the perspective of watershed spatial structure based on digital elevation models," *Remote Sensing*, vol. 13, no. 19, p. 3926, 2021.
- [22] R. MacMillan and P. Shary, "Chapter 9 landforms and landform elements in geomorphometry," in *Geomorphometry*, ser. Developments in Soil Science, T. Hengl and H. I. Reuter, Eds. Elsevier, 2009, vol. 33, pp. 227–254. [Online]. Available: <https://www.sciencedirect.com/science/article/pii/S0166248108000093>
- [23] G. Miliareis and D. Argialas, "Segmentation of physiographic features from the global digital elevation model/gtopo30," *Computers & Geosciences*, vol. 25, no. 7, pp. 715–728, 1999. [Online]. Available: <https://www.sciencedirect.com/science/article/pii/S0098300499000254>
- [24] M. Mokarram and D. Sathyamoorthy, "A review of landform classification methods," *Spatial Information Research*, vol. 26, pp. 647–660, 2018.
- [25] M. W. Ngunjiri, Z. Libohova, P. R. Owens, and D. G. Schulze, "Landform pattern recognition and classification for predicting soil types of the usasini gishu plateau, kenya," *CATENA*, vol. 188, p. 104390, 2020. [Online]. Available: <https://www.sciencedirect.com/science/article/pii/S0341816219305326>
- [26] G. Pau, F. Fuchs, O. Sklyar, M. Boutros, and W. Huber, "EBIImage—an R package for image processing with applications to cellular phenotypes," *Bioinformatics*, vol. 26, no. 7, pp. 979–981, 03 2010. [Online]. Available: <https://doi.org/10.1093/bioinformatics/btq046>
- [27] QGIS.org, "Qgis geographic information system," 2022. [Online]. Available: <https://www.qgis.org/>
- [28] E. Ricci and R. Perfetti, "Retinal blood vessel segmentation using line operators and support vector classification," *IEEE Transactions on Medical Imaging*, vol. 26, no. 10, pp. 1357–1365, 2007.
- [29] J. Serra, "Introduction to mathematical morphology," *Computer Vision, Graphics, and Image Processing*, vol. 35, no. 3, p. 283–305, 1986.
- [30] R. K. Straumann and R. S. Purves, "Delineation of valleys and valley floors," in *Proceedings of the 5th International Conference on Geographic Information Science*, ser. GIScience '08. Berlin, Heidelberg: Springer-Verlag, 2008, p. 320–336.

- [31] Y. Sun, A. K. C. Wong, and M. S. Kamel, "Classification of imbalanced data: A review," *International Journal of Pattern Recognition and Artificial Intelligence*, vol. 23, no. 04, pp. 687–719, 2009. [Online]. Available: <https://doi.org/10.1142/S0218001409007326>
- [32] A. Sărăsan, E. Józsa, A. C. Ardelean, and L. Drăgut, "Sensitivity of geomorphons to mapping specific landforms from a digital elevation model: A case study of drumlins," *Area*, vol. 51, no. 2, p. 257–267, 2018.
- [33] X. Tan and B. Triggs, "Enhanced local texture feature sets for face recognition under difficult lighting conditions," in *International workshop on analysis and modeling of faces and gestures*. Springer, 2007, pp. 168–182.
- [34] E. Toulia, E. Kokinou, and C. Panagiotakis, "The contribution of pattern recognition techniques in geomorphology and geology: the case study of tinos island (cyclades, aegean, greece)," *European Journal of Remote Sensing*, vol. 51, no. 1, pp. 88–99, 2018. [Online]. Available: <https://doi.org/10.1080/22797254.2017.1405716>
- [35] L.-Y. Xiong, A.-X. Zhu, L. Zhang, and G.-A. Tang, "Drainage basin object-based method for regional-scale landform classification: a case study of loess area in china," *Physical Geography*, vol. 39, no. 6, pp. 523–541, 2018. [Online]. Available: <https://doi.org/10.1080/02723646.2018.1442062>
- [36] G. Yan, H. Cheng, L. Teng, W. Xu, Y. Jiang, G. Yang, and Q. Zhou, "Analysis of the use of geomorphic elements mapping to characterize subaqueous bedforms using multibeam bathymetric data in river system," *Applied Sciences*, vol. 10, no. 21, 2020. [Online]. Available: <https://www.mdpi.com/2076-3417/10/21/7692>

ACKNOWLEDGMENT

The acknowledge the support from CONACYT with Cátedra-CONACYT 7795 and Cátedra-CONACYT 7308.